BBA - Bioenergetics 1859 (2018) 806–816

Contents lists available at ScienceDirect

BBA - Bioenergetics

journal homepage: www.elsevier.com/locate/bbabio

Post-translational modifications of VDAC1 and VDAC2 cysteines from rat liver mitochondria☆

Rosaria Saletti[a,1], Simona Reina[b,c,1], Maria G.G. Pittalà[c,d], Andrea Magrì[b,c,d], Vincenzo Cunsolo[a], Salvatore Foti[a,*], Vito De Pinto[c,d,**]

[a] Department of Chemical Sciences, Organic Mass Spectrometry Laboratory, University of Catania, Viale A. Doria 6, 95125 Catania, Italy
[b] Department of Biological, Geological and Environmental Sciences, Section of Molecular Biology, University of Catania, Viale A. Doria 6, 95125 Catania, Italy
[c] National Institute for Biomembranes and Biosystems, Section of Catania, Viale A. Doria 6, 95125 Catania, Italy
[d] Department of Biomedicine and Biotechnology, Section of Biology and Genetics, Viale A. Doria 6, 95125, Catania, Italy

ARTICLE INFO

Keywords:
Cysteine over-oxidation
Orbitrap fusion tribrid
Mitochondria
Mitochondria quality control
ROS
Hydroxyapatite

ABSTRACT

VDACs three isoforms (VDAC1, VDAC2, VDAC3) are integral proteins of the outer mitochondrial membrane whose primary function is to permit the communication and exchange of molecules related to the mitochondrial functions. We have recently reported about the peculiar over-oxidation of VDAC3 cysteines. In this work we have extended our analysis, performed by tryptic and chymotryptic proteolysis and UHPLC/High Resolution ESI-MS/MS, to the other two isoforms VDAC1 and VDAC2 from rat liver mitochondria, and we have been able to find also in these proteins over-oxidation of cysteines. Further PTM of cysteines as succination has been found, while the presence of selenocysteine was not detected. Unfortunately, a short sequence stretch containing one genetically encoded cysteine was not covered both in VDAC2 and in VDAC3, raising the suspect that more, unknown modifications of these proteins exist. Interestingly, cysteine over-oxidation appears to be an exclusive feature of VDACs, since it is not present in other transmembrane mitochondrial proteins eluted by hydroxyapatite. The assignment of a functional role to these modifications of VDACs will be a further step towards the full understanding of the roles of these proteins in the cell.

1. Introduction

In the outer mitochondrial membrane of all eukaryotes, VDACs (Voltage Dependent Anion Selective Channel) are the main responsible for the cross-talk between the organelle and the rest of the cell [1, 2]. As aqueous channels, VDACs mediate the transport of ions and metabolites across the OMM. In addition, the interactions of VDACs with several cytoplasmic proteins like hexokinase [3] tubulin [4, 5], dynein [6], actin [7], synuclein [8], mutated forms of SOD1 [9], pro-apopototic and antiapoptotic factors [10, 11], highlight a crucial function of VDAC in several biological processes ranging from mitochondrial bioenergetics to apoptosis. In mammals, the presence of three isoforms (VDAC1-VDAC2-VDAC3) with a relatively high sequence similarity and structural homology, contrasts with the different roles that have been proposed within the cell. Indeed, along with their common involvement in cellular bioenergetics maintenance, VDAC1 and VDAC2 have been proposed to have opposite functions in programmed cell death (pro-apoptotic the first one [2, 10, 12] and anti-apoptotic the second one [13]), while recent evidences suggest VDAC3 as a player in ROS metabolism control [14, 15].

The three-dimensional structure obtained by NMR and X-ray crystallography techniques [16–18] revealed VDAC1 as a transmembrane β-barrel containing an α-helix N-terminal segment that, according to the protein arrangement within the membrane [19], protrudes towards the cytosol. Interestingly, the high sequence similarity with the other two isoforms suggests the existence of a common structural pattern in the pore organization, as confirmed by the crystallographic structure resolved for VDAC2 from zebrafish [20] and the in silico prediction of

Abbreviations: VDAC, voltage-dependent anion selective channel; OMM, outer mitochondrial membrane; PTM, post-translational modification; ROS, reactive oxygen species; MS, mass spectrometry; HTP, hydroxyapatite

☆ This article is part of a Special Issue entitled 20th European Bioenergetics Conference, edited by László Zimányi and László Tretter.

* Correspondence to: V. De Pinto, Department of Biomedicine and Biotechnology, Section of Biology and Genetics, University of Catania, Campus S. Sofia, Building 2, Viale A. Doria 6, 95125 Catania, Italy.

** Correspondence to: S. Foti, Department of Chemical Sciences, Organic Mass Spectrometry Laboratory, University of Catania, Campus S. Sofia, Building 1, Viale A. Doria 6, 95125 Catania, Italy.

E-mail addresses: rsaletti@unict.it (R. Saletti), vcunsolo@unict.it (V. Cunsolo), sfoti@unict.it (S. Foti), vdpbiofa@unict.it (V. De Pinto).

[1] These authors equally contributed to the article.

https://doi.org/10.1016/j.bbabio.2018.06.007
Received 3 February 2018; Received in revised form 4 June 2018; Accepted 7 June 2018
Available online 08 June 2018

human VDAC3 structure [15].

It is widely reported that in its native environment, VDAC exhibits several post-translational modifications such as phosphorylation [21], acetylation [22], tyrosine nitration [23] whose role in protein activity has been only partially clarified. For instance, VDAC1 phosphorylation has been associated to the modulation of channel gating properties [24], prevention of cell death [25], sensitization to apoptosis [26, 27] and/or various physiopathological conditions [28]. However, information regarding the modifications of sulfur-containing amino acids is rather limited. It is known, for example, that S-nitrosylation of VDAC modulates sperm function [29] and correlates with enhanced calcium-induced mitochondrial swelling and cytochrome *c* release [30]. Given the emerging role of redox signaling in numerous cellular processes [31] we focused on unraveling the modifications of VDAC's cysteine and methionine residues under physiological conditions. Through the combination of the UHPLC/High Resolution ESI MS/MS with the "in-solution" digestion of VDACs purified from rat liver mitochondria, we recently succeeded in defining a complete and detailed profile of oxidations of VDAC3 cysteines and methionines [32], discovering that cysteines may reside in a wide range of oxidation states. In this work, we thus report for the first time an accurate survey of the oxidative states of sulfur containing amino acids of VDAC1 and VDAC2 isolated from rat liver mitochondria. As for VDAC3, we found cysteines over-oxidized to sulfonic acid also in VDAC1 and VDAC2. A comparison with highly hydrophobic mitochondrial proteins eluted from hydroxyapatite shows that this modification happens specifically in VDAC isoforms. To complete the survey of the most common cysteine modifications, also the presence of succination (i.e. the addition of fumarate to reduced cysteines) and selenocysteine was examined in the three isoforms VDAC1–3. Possible consequence or a rationale of such VDAC modifications in the cell context is discussed.

2. Materials and methods

2.1. Chemicals

All chemicals were of the highest purity commercially available and were used without further purification. Ammonium bicarbonate, TrisHCl, Triton X-100, Sucrose, EDTA, HEPES, formic acid (FA), phenylmethylsulfonyl fluoride (PMSF), dithiothreitol (DTT), iodoacetamide (IAA) and chymotrypsin were obtained from Sigma-Aldrich (Milan, Italy). Modified porcine trypsin was purchased from Promega (Madison, WI, USA). Water and acetonitrile (OPTIMA® LC/MS grade) for LC/MS analyses were provided from Fisher Scientific (Milan, Italy).

2.2. Isolation of intact rat liver mitochondria and proteins reduction and alkylation

Rat liver mitochondria were prepared as already reported [33, 34]. Briefly, 5 livers of male Sprague-Dawley rats weighing 300–500 g (Envigo) were resuspended into buffer A (0.25 M sucrose, 10 mM HEPES, 0.1 mM EDTA, 0.15 μM PMSF, pH 7.0) in ratio (v/w) 3:1 and homogenized with a glass Potter-Elvehjem pestle. Homogenate was diluted 1:1 (v/v) in buffer A and centrifuged for 5 min at 1000 ×*g* at 4 °C. After repeating this step on the pellet obtained in the first homogenization, the supernatants were reunited and subjected to differential centrifugations. Final mitochondria-enriched fraction was resuspended in buffer B (sucrose 0.25 M, HEPES 10 mM, 0.15 μM PMSF) and total yield was determined by micro-Lowry method. Reduction/alkylation was carried on before VDACs purification in order to avoid any possible artifacts due to air exposure. 70 mg of intact mitochondria were incubated for 3 h at 4 °C in Tris-HCl 10 mM (pH 8.3) containing 0.7 mmol of DTT, which corresponds to an excess in the order of 50:1 (mol/mol) over the estimated thiol groups. The temperature was kept at 4 °C in order to avoid possible reduction of methionine sulfoxide to methione by methionine sulfoxide reductase. After centrifugation for 30 min at 10,000 ×*g* at 4 °C, alkylation was performed by addition of iodoacetamide at the 2:1 M ratio over DTT for 1 h in the dark at 25 °C. Mixture was centrifuged for 30 min at 10,000 ×*g* at 4 °C and the pellet was stored at −80 °C until further use.

2.3. Preparation of VDAC1 and VDAC2 enriched fractions from rat liver mitochondria

VDAC1 and VDAC2 were purified from rat liver mitochondria as in [32]. 70 mg of reduced and alkylated intact mitochondria were lysed in buffer A (10 mM TrisHCl, 1 mM EDTA, 3% Triton X-100, pH 7.0) in ratio 5:1 (mitochondria mg/buffer volume) [33] for 30 min on ice and centrifuged at 17,400 ×*g* for 30 min at 4 °C. The supernatant containing mitochondrial proteins was subsequently divided onto 12 glass Econo-column 2.5 × 30 cm (Biorad), each packed with 0.6 g of dry hydroxyapatite (Bio-Gel HTP, Biorad). Columns were eluted with 5 mL of buffer A at 4 °C and fractions from each column were collected and precipitated with 9 volumes of cold acetone at −20 °C.

2.4. In-solution digestion of the hydroxyapatite eluate

Pellets from the hydroxyapatite eluate was purified from non-protein contaminating molecules with the PlusOne 2-D Clean-Up kit (GE Healthcare Life Sciences, Milan, Italy) according to the manufacturer's recommendations. The desalted protein pellet obtained was suspended in 100 μL of 50 mM ammonium bicarbonate (pH 8.3) and incubated at 4 °C for 15 min. After, 100 μL of 0.2% RapiGest SF (Waters, Milan, Italy) in 50 mM ammonium bicarbonate were added and the sample was put at 4 °C for 30 min. Protein amount, determined using fluorometer assay kit, resulted 1 μg (Invitrogen Qubit™ Protein Assay kit, ThermoFisher Scientific, Milan, Italy). The reduction was carried out by adding 2.6 μg of DTT dissolved in the same buffer for 3 h in the dark at 25 °C. Subsequently, alkylation was performed by addition of iodoacetamide at the same molar ratio over total thiol groups and the reaction allowed to proceed for 1 h in the dark at 25 °C. Finally, reduced and alkylated proteins were subjected to digestion using modified porcine trypsin or chymotrypsin in ammonium bicarbonate (pH 8.3) at an enzyme-substrate ratio of 1:50 and 1:25, respectively, at 37 °C for 4 h. The protein digests were then dried under vacuum, dissolved in 20 μL of 5% FA and analyzed by nano UHPLC/High Resolution ESI-MS/MS.

2.5. Liquid chromatography and tandem mass spectrometry (LC–MS/MS) analysis

Mass spectrometry data were acquired on an Orbitrap Fusion Tribrid (Q-OT-qIT) mass spectrometer (ThermoFisher Scientific, Bremen, Germany) equipped with a ThermoFisher Scientific Dionex UltiMate 3000 RSLCnano system (Sunnyvale, CA).

Samples obtained by in-solution digestion were reconstituted in 20 μL of 5% FA aqueous solution and 1 μL was loaded onto an Acclaim®Nano Trap C18 column (100 μm i.d. × 2 cm, 5 μm particle size, 100 Å). After washing the trapping column with solvent A (H_2O + 0.1% FA) for 3 min at a flow rate of 7 μL/min, the peptides were eluted from the trapping column onto a PepMap® RSLC C18 EASY-Spray, 75 μm × 50 cm, 2 μm, 100 Å column and were separated by elution at a flow rate of 0.250 μL/min, at 40 °C, with a linear gradient of solvent B in A from 5% to 20% in 32 min, followed by 20% to 40% in 30 min, and 40% to 60% in 20 min.

Eluted peptides were ionized by a nanospray (Easy-spray ion source, Thermo Scientific) using a spray voltage of 1.7 kV and introduced into the mass spectrometer through a heated ion transfer tube (275 °C). Survey scans of peptide precursors in the *m/z* range 400–1600 were performed at resolution of 120,000 (@ 200 *m/z*) with a AGC target for Orbitrap survey of 4.0×10^5 and a maximum injection time of 50 ms. Tandem MS was performed by isolation at 1.6 Th with the quadrupole, and high energy collisional dissociation (HCD) was performed in the

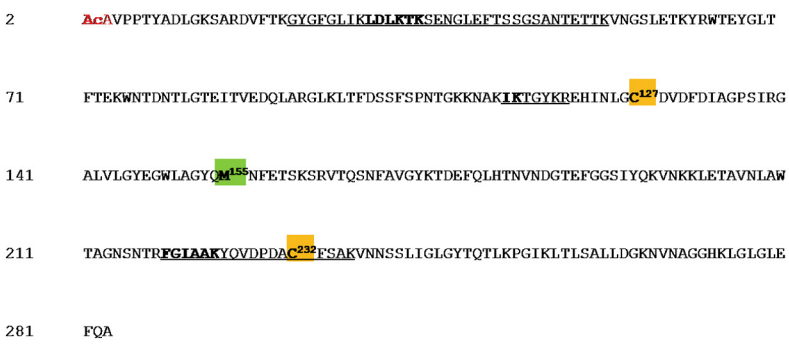

Fig. 1. Sequence coverage map of rVDAC1 obtained by tryptic digestion. Solid lines indicate unique tryptic peptides originated by missed-cleaveges, used to cover sequences shared by isoforms. Sequences shared by isoforms are reported in bold. The oxidized cysteine residues are highlighted in yellow and the oxidized methionine residues are highlighted in green. The N-terminal acetylated alanine is shown in red.

Ion Routing Multipole (IRM), using a normalized collision energy of 35 and rapid scan MS analysis in the ion trap. Only those precursors with charge state 1–4 and an intensity above the threshold of $5{\cdot}10^3$ were sampled for MS^2. The dynamic exclusion duration was set to 60 s with a 10 ppm tolerance around the selected precursor and its isotopes. Monoisotopic precursor selection was turned on. AGC target and maximum injection time (ms) for MS/MS spectra were 1.0×10^4 and 100, respectively. The instrument was run in top speed mode with 3 s cycles, meaning the instrument would continuously perform MS^2 events until the list of non-excluded precursors diminishes to zero or 3 s, whichever is shorter. MS/MS spectral quality was enhanced enabling the parallelizable time option (i.e. by using all parallelizable time during full scan detection for MS/MS precursor injection and detection).

Mass spectrometer calibration was performed using the Pierce® LTQ Velos ESI Positive Ion Calibration Solution (Thermo Fisher Scientific). MS data acquisition was performed using the *Xcalibur* v. 3.0.63 software (Thermo Fisher Scientific).

2.6. Database search

LC–MS/MS data were processed by Proteome Discoverer v. 1.4.1.14 (Thermo Scientific) and PEAKS software (v. 8.5, Bioinformatics Solutions Inc., Waterloo, ON Canada). Data were searched against the SwissProt database (release July 2016, containing 550,552 entries) using the MASCOT algorithm (Matrix Science, London, UK, version 2.5.1). The search was performed against *rattus* sequences database (7961 sequences). Full tryptic or chymotrypsin peptides with a maximum of 3 missed cleavage sites were subjected to bioinformatic search. Cysteine carboxyamidomethylation was set as fixed modification, whereas acetylation of protein N-terminal, trioxidation and succination of cysteine, presence of selenocysteine, oxidation of methionine, and transformation of N-terminal glutamine and N-terminal glutamic acid residue in the pyroglutamic acid form were included as variable modifications. The precursor mass tolerance threshold was 10 ppm and the max fragment mass error was set to 0.6 Da. Peptide spectral matches (PSM) were validated using Target Decoy PSM Validator node based on q-values at a 1% FDR.

Identification of the other transmembrane mitochondrial proteins eluted by hydroxyapatite was obtained using Proteome Discoverer v. 1.4.1.14 software with the following filters: Mascot significance threshold 0.05; peptide confidence: high; peptide score: > 20. A protein was considered identified with minimum of two peptides.

3. Results

3.1. Mass spectrometric analysis of VDAC1 from rat liver mitochondria

In this work, the primary structure of VDAC1 from *Rattus norvegicus* (rVDAC1) has been investigated by tryptic and proteinase K digestion, and MALDI and ESI-MS/MS mass spectrometric analysis [35]. When combining the coverage obtained in all the experiments, a total coverage of 99% (279 of 282 amino acids) was achieved. The N-terminal methionine was never found, indicating that it is removed during protein maturation. The protein tract not covered in this analysis included the sequence Gly^{94}-Lys^{96}.

To exclude the possibility that any unspecific and undesired oxidation could happen during the purification protocol, we added DTT to the buffer used to suspend the mitochondria and in the purification steps, as described in the Experimental Section. In-solution tryptic digestion of the hydroxyapatite (HTP) eluate of Triton X-100 and mass spectrometry analysis was then performed. Note that in this experiment every protein present in the HTP eluate was digested, producing a very complex peptide mixture. rVDAC1 peptides found in the analysis of mitochondria lysate incubated with DTT are reported in Supplementary Table 1.

UHPLC/High Resolution ESI-MS/MS of the tryptic digest allowed the coverage of 100% of the rVDAC1 sequence (Fig. 1 and Supplementary Table 1), thus chymotryptic digestion was not required. Although some predicted tryptic peptides of the rVDAC1 sequence are shared by two or three isoforms, unequivocal sequence coverage was obtained by the detection of unique peptides originated by missed-cleavages. The sequences of these unique peptides are underlined in Fig. 1.

The results also confirmed that the N-terminal Met, reported in the SwissProt database sequence (Acc. N. Q9Z2L0), is absent in the mature protein and that the N-terminal Ala is almost totally present in the acetylated form (Supplementary Fig. 1, Supplementary Table 1, fragments 2 and 3).

Data analysis was particularly focused on the investigation of the oxidation state of Met and Cys residues. The sequence of rat VDAC1 comprises one methionine in position 155, and two cysteines in position 127 and 232. It should be noted that the numeration adopted in the discussion starts from Met^1, which, actually, has been found to be absent.

Among the peptides identified, besides the fragment containing Met^{155} in the normal form (Supplementary Table 1, fragment 26), a peptide with this residue in the form of methionine sulfoxide was also detected (Supplementary Table 2, fragment 3).

The full scan and fragment ion mass spectrum of the molecular ion of the peptide G^{140}ALVLGYEGWLAGYQMNFETSK^{161} with Met^{155} as methionine sulfoxide are reported in Supplementary Fig. 2. The MS/MS spectrum presents the characteristic neutral loss of 64 Da corresponding to the ejection of methanesulfenic acid from the side chain of MetO [36].

Although from these data a precise determination of the amount of methionine and methionine sulfoxide respectively present in the digestion mixture cannot be obtained, a rough estimation of their relative abundance can be derived from the comparison of the absolute intensities of the multiply charged molecular ions of the respective peptides. These calculations for the doubly charged molecular ion of the fragment G^{140}-K^{161}, detected in the tryptic digest, indicate a ratio of 65:1 MetO/Met (Table 1).

Analysis of the mass spectral data oriented to the determination of

Table 1
Comparison of the absolute intensities of molecular ions of selected sulfur containing tryptic peptides found in the analysis of rVDAC1 reduced with DTT, carboxyamidomethylated and digested in-solution. The ratio reported was determined from a single experiment.

Peptide	Position in the sequence	Measured monoisotopic *m/z*	Absolute intensity	Ratio Ox/Red
EHINLG**C**DVDFDIAGPSIR	121–139	1059.9929 (+2)	$1.10 \cdot 10^6$	0.12
EHINLG***C***DVDFDIAGPSIR		710.0099 (+3)	$9.10 \cdot 10^6$	
EHINLG**C**DVDFDIAGPSIR	121–139	1050.9885 (+2)	$1.62 \cdot 10^6$	0.26
EHINLG***C***DVDFDIAGPSIR		1055.5061 (+2)	$6.19 \cdot 10^6$	
GALVLGYEGWLAGYQ**M**NFETSK	140–161	1225.5898 (+2)	$1.07 \cdot 10^7$	65
GALVLGYEGWLAGYQMNFETSK		1217.5914 (+2)	$1.64 \cdot 10^5$	
YQVDPDA**C**FSAK	225–236	696.2938 (+2)	$4.18 \cdot 10^6$	0.1
YQVDPDA***C***FSAK		700.8118 (+2)	$4.06 \cdot 10^5$	

M: methionine sulfoxide; ***C***: cysteine carboxyamidomethylated; **C**: cysteine oxidized to sulfonic acid. **E**: pyroglutamic acid form.

oxidation state of cysteines showed that for both the cysteines 127 and 232, besides the peptides containing these residues carboxyamidomethylated (Supplementary Table 1, fragments 23, 24, 25, 33, and 34), peptides with these amino acids in the form of sulfonic acid were also identified (Fig. 2, Supplementary Table 2, fragments 1, 2 and 4).

Again, a rough estimation of the relative abundance of the cysteines oxidized to sulfonic acid with respect to the Cys in the carboxyamidomethylated form can be derived from the ratio of the absolute intensities of the multiply charged molecular ions of the corresponding peptides. From these comparisons (Table 1), a ratio Cys-oxidized-to-sulfonic-acid/Cys-carboxyamidomethylated ranging from about 0.1:1 to 0.26:1 is observed. In the evaluation of these results, it should be considered that the oxidation of cysteine to cysteine sulfonic acid introduces a strong negative charge in the peptide, thus hampering the formation of positive ions. However, even taking into account these considerations, the data in Table 1 suggest that a sizeable amount of cysteines is oxidized to sulfonic acid.

3.2. Mass spectrometric analysis of VDAC2 from rat liver mitochondria

3.2.1. Tryptic digestion

As for rVDAC1, also the sequence of VDAC2 from *Rattus norvegicus* (rVDAC2) has been characterized by tryptic and proteinase K digestion, and MALDI and ESI-MS/MS mass spectrometric analysis [35] reaching a total coverage of 89,5% (263 of 294 amino acids). The N-terminal methionine was found to be removed in the mature protein and the region Gly^{138}-Thr^{168} was not covered.

In our work, the analysis of tryptic digest of the hydroxyapatite eluate of Triton X-100 solubilized rat liver mitochondria analyzed by UHPLC/High Resolution ESI-MS/MS allowed to identify 84.35% of the protein (248 of 294 amino acids) (Fig. 3 and Supplementary Table 3).

Although some predicted tryptic peptides of the rVDAC2 sequence are shared by two or three isoforms, unequivocal sequence coverage was obtained by the detection of unique peptides originated by missed-cleavages.

Also in rVDAC2, the N-terminal methionine, reported in the SwissProt database sequence (Acc. N. P81155), was found to be absent and the Ala^2 resulted present in the acetylated form (Supplementary Table 3, fragment 1 and Supplementary Fig. 3).

In the rVDAC2 there are one methionine in position 167, and eleven cysteines in position 4, 5, 9, 14, 48, 77, 104, 134, 139, 211, and 228. The oxidation state of the Met residue could not be determined in the analysis of the tryptic digest because the peptide containing the Met residue was not found. Instead, the partial oxidation of Cys^{48} (Table 2 and Fig. 4), Cys^{77}, Cys^{104}, Cys^{211}, and Cys^{228} (Supplementary Table 4, fragments 1–6 and Supplementary Figs. 4–6) to sulfonic acid, and the presence of the cysteines 4, 5, 9, and 14 exclusively in the carboxyamidomethylated form was detected (Supplementary Table 3, fragment 1, and Supplementary Fig. 3).

The relative abundance of the peptides containing the cysteines oxidized to sulfonic acid in comparison with peptides containing "normal" cysteines (i.e. carboxyamidomethylated cysteines), was estimated from the ratio of the absolute intensities of the respective multiply charged molecular ions. Table 2 shows that the cysteines 48 and 77 are oxidized to sulfonic acid in considerable amount, whereas cysteines 104, 211 and 228 oxidized to sulfonic acid are present only in trace amount.

Peptides including Cys^{134} and Cys^{139} resulted undetectable, so it was not possible to evaluate their oxidation state.

3.2.2. Chymotryptic digestion

To increase the sequence coverage, chymotryptic digestion of rVDAC2 was also performed. When combining the results obtained in the tryptic and chymotryptic digestions, the coverage of the sequence of rVDAC2 was extended to 96, 26% (283 out of 294 amino acids) (Fig. 3 and Supplementary Tables 3, 5). Although some predicted chimotryptic peptides of the rVDAC2 sequence are shared by two or three isoforms, unequivocal sequence coverage was obtained by the detection of unique peptides originated by missed-cleavages, except for the sequence GYEGWLAGY, which was not possible to cover by unique peptides (shown in bold in Fig. 3).

The region still not covered corresponds to the sequence Glu^{133}-Phe^{143}, a part of the stretch not determined in a previous work [35] (Fig. 5). In the chymotryptic digest, Met^{167} was identified either as normal methionine (Supplementary Table 5, fragments 12 and 13) and as methionine sulfoxide (Supplementary Table 6, fragments 1 and 2 and Supplementary Fig. 7). Because the peptide LAGYQM is shared by all the three isoforms, a rough estimation of the Ox/Red Ratio can be derived from the comparison of the absolute intensities of the multiply charged molecular ions of the peptide **QM**TFDSAKSKL, which is unique of the rVDAC2 sequence. As shown in Table 3, the two forms appear present in approximately equal amounts. Instead, cysteines oxidized to sulfonic acid were undetectable. (See Fig. 5.)

3.3. Presence of selenocysteines and identification of succination in VDAC isoforms

Mass spectral data were also analyzed in order to detect the presence of selenocysteines and the occurence of cysteine succination. Selenocysteines were not observed in all the rVDAC isoforms. Succinated cysteines were not found in rVDAC1, whereas in rVDAC2 only Cys48 was identified as succinated in very low amount (Supplementary Table 7 and Supplementary Fig. 8) (Table 4). In rVDAC3 three cysteines (8, 36 and 229) were succinated (Supplementary Table 8 and Supplementary Fig. 9), with two of them (36 and 229) in very low amounts (Table 5).

3.4. No other protein carrying over-oxidized cysteine was identified in mitochondrial HTP eluates

Many works have outlined the power of HTP as a chromatographic

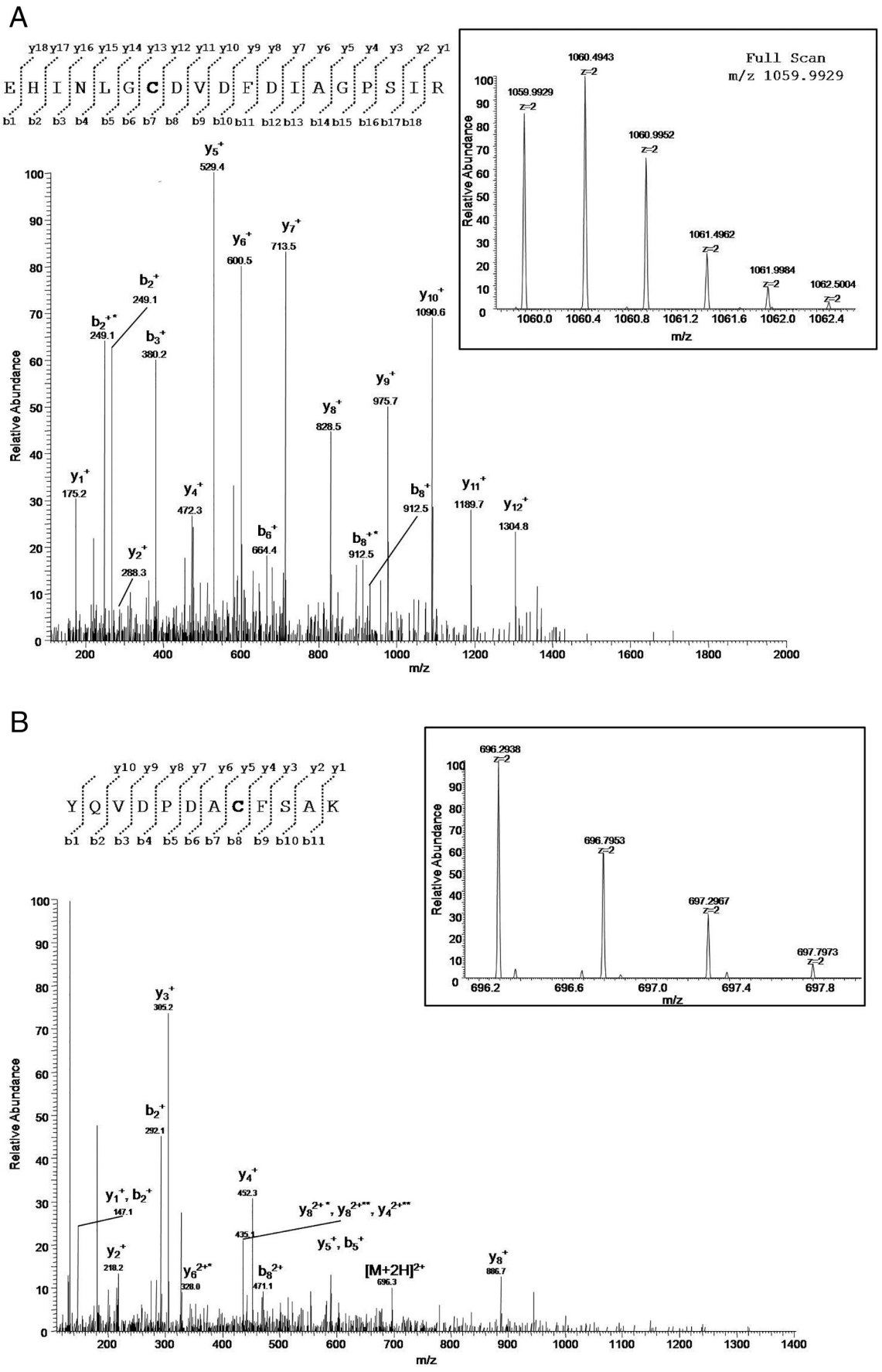

(caption on next page)

Fig. 2. Top: MS/MS spectrum of the doubly charged molecular ion at *m/z* 1059.9929 (calculated 1059.9919) of the VDAC1 tryptic peptide from *Rattus norvegicus* containing cysteine residue 127 in the form of sulfonic acid. Bottom: MS/MS spectrum of the doubly charged molecular ion at *m/z* 696.2938 (calculated 696.2938) of the VDAC1 tryptic peptide from *Rattus norvegicus* containing cysteine residue 232 in the form of sulfonic acid. The insets show the full scan mass spectrum of molecular ions. Fragment ions originated from the neutral loss of H_2O are indicated by an asterisk. Fragment ions originated from the neutral loss of NH_3 are indicated by two asterisks.

matrix able to selectively allow the purification of integral membrane proteins. This was also proved true for VDACs [33, 34]. Consequently, the HTP eluate from Triton X-100 solubilized rat liver mitochondria has been the starting material for the preparations used in this work. The HTP eluate (or pass-through, since the analyzed proteins are only those not retained by the chromatography) results enriched in VDAC isoforms, but many other proteins are also present. The power of the deep Mass Spectrometric analysis reported us a list of other proteins, identified by the concordance between the peptide masses and the sequences in the databases (Table 6). We were interested to know whether other mitochondrial membrane proteins carried similar over-oxidations as those found in VDAC3 [32]. Although in some of the proteins reported in Table 6 (shown in bold) tryptic peptides containing cysteines residues were identified, no evidence of over-oxidized cysteines was found. This is a strong indication that the cysteine over-oxidation in the inter-membrane space is peculiar of VDACs. Instead, several of the proteins reported Table 6 present methionines in the oxidized form.

Among the other proteins found in the HTP pass-through, and not being transmembrane proteins, only the mitochondrial matrix protein thiosulfate sulfur-transferase (UniProtKB - P24329), the mitochondrial import factor for the cytosolic 5S rRNA, was reported to be oxidized from our analysis, outlining how rare and peculiar is this modification.

4. Discussion

Using the same techniques that allowed the deep characterization of human and rat VDAC3 [32], we succeeded in obtaining a good sequence coverage of VDAC1 and VDAC2 from rat liver mitochondria, together with the accurate determination of the oxidative states of their cysteine and methionine residues. The association of the "in-solution" digestion of the eluates obtained from hydroxyapatite chromatography with the high-resolution mass spectrometry has indeed permitted to overcome the remarkable difficulties associated with the analysis of membrane proteins. In particular, it is worth to note that the digestion in solution of the HTP eluate allowed bypassing the SDS-electrophoresis step with its potential dangers of unwanted oxidations. Unfortunately, even though the techniques applied are the most updated available, it is striking that a short amino acid stretch in the sequences of both VDAC2 and VDAC3 could not be identified, leaving a small leak in the sequence coverage of the two proteins (Fig. 5). Interestingly these two short stretches do contain a cysteine and are located in a very close position with respect to the whole sequences. Although it is possible that peptides present in the digested mixture may remain undetected in the mass spectrometric analysis, it is tempting to speculate that parts of sequences not matched by the mass spectral data hide sequence modifications, presently unknown but possibly of structural and functional importance.

4.1. VDAC1 and VDAC2 show evidence of oxidized sulfur-containing amino acids

A particularly intriguing result was the identification, also in VDAC isoforms 1 and 2, of oxidized methionines and of cysteine residues over-oxidized up to sulfonic acid, an irreversible state, at least in the cell, of the sulfur-containing amino acid. These modifications, affecting cysteines 127 and 232 in rVDAC1, and 48, 77, 104, 211, and 228 in rVDAC2, respectively, are however, present in relatively smaller amount than in rVDAC3, previously characterized [32]. There are interesting differences among the cysteine oxidation patterns affecting the VDAC isoforms.

In the case of VDAC1 the only two cysteine residues in the sequences are not either close one another nor in a highly hydrophilic environment (see the 3D structure of the protein in Fig. 6). However, in the physiological state, a consistent amount of cysteines in VDAC1 is present in the reduced form or can be involved in disulfide bridges formation, which, if present, must be necessarily intermolecular in nature, owing to the position of the two cysteines in the protein. VDAC1 sulfur residues do not play any special function in the protein pore-forming activity.

VDAC2 is particularly rich of cysteines. In the rat there is the highest number of cysteines, 11 against 9 in human and mouse. In the critical N-terminal sequence, or very close to it, there is an abundance of 4 cysteines very much clustered. It is very indicative that these cysteines, in our analysis, did not show any presence of oxidization, i.e. they were found as carboxymethylated residues: in chemical terms this means that these cysteines are in a reversible oxidation state, i.e. they can oscillate between a reduced and a mild oxidized state, like in the case of disulfide bridge formation. In the remaining sequence four cysteine containing peptides were detected and they were found both over-oxidized and reduced. A rough estimation of the ratio between the two peptides was attempted, with the aim to get at least a broad indication of the amount of cysteines found in any oxidized or reduced state. From this survey (see Table 2) Cys 48 and Cys 77 were present in an approximately 1:10 ratio oxidized/reduced, while Cys 104 and Cys 211/228, both on the same peptide, had a rough ratio of 1:100 oxidized/reduced, i.e. the reduced state is more an exception than a rule. Cys 134 and Cys 139 are on a sequence stretch that was not detected, and it thus presently impossible to state their oxidation state (discussed above).

In front of these results, in rat VDAC3 we found that four cysteines

Fig. 3. Sequence coverage map of rVDAC2 obtained by enzymatic digestions. Solid lines indicate the coverage obtained with tryptic peptides; dotted lines the coverage obtained with chymotryptic peptides. The sequence stretch not covered by unique peptides is reported in bold. The carboxyamidomethylated cysteine residues are highlighted in gray; the oxidized cysteine residues are highlighted in yellow and the oxidized methionine residues are highlighted in green. The N-terminal acetylated alanine is shown in red.

Table 2
Comparison of the absolute intensities of molecular ions of selected sulfur containing tryptic peptides found in the analysis of rVDAC2 reduced with DTT, carboxyamidomethylated and digested in-solution. The ratio reported was determined from a single experiment.

Peptide	Position in the sequence	Measured monoisotopic *m/z*	Absolute intensity	Ratio Ox/Red
TKS**C**SGVEFSTSGSSNTDTGK	45–65	1064.4547 (+2)	$5.01{\cdot}10^4$	0.08
TKS***C***SGVEFSTSGSSNTDTGK		712.9837 (+3)	$6.03{\cdot}10^5$	
S**C**SGVEFSTSGSSNTDTGK	47–65	949.8823 (+2)	$1.09{\cdot}10^5$	0.41
S***C***SGVEFSTSGSSNTDTGK		954.4005 (+2)	$2.67{\cdot}10^5$	
YKW**C**EYGLTFTEK	74–86	858.3899 (+2)	$7.98{\cdot}10^4$	0.75
YKW***C***EYGLTFTEK		862.9038 (+2)	$1.06{\cdot}10^5$	
W**C**EYGLTFTEK	76–86	712.8052 (+2)	$1.22{\cdot}10^5$	0.030
W***C***EYGLTFTEK		717.3243 (+2)	$4.05{\cdot}10^6$	
WNTDNTLGTEIAIEDQI**C**QGLK	87–108	1255.5902 (+2)	$9.98{\cdot}10^4$	0.007
WNTDNTLGTEIAIEDQI***C***QGLK		1260.1088 (+2)	$1.36{\cdot}10^7$	
V**C**EDFDTSVNLAWTSGTN**C**TR	210–230	1207.9841 (+2)	$3.16{\cdot}10^4$	0.008
V***C***EDFDTSVNLAWTSGTN***C***TR		1217.0264 (+2)	$3.90{\cdot}10^6$	

C: cysteine carboxyamidomethylated; **C**: cysteine oxidized to sulfonic acid.

upon six detected (Cys 36, 65, 165, and 229) are oxidized to sulfonic acid in a considerable amount [32] and Cys 2 and Cys 8 were not heavily oxidized, showing instead carboxyamidation and thus the possibility of a reduced and mildly oxidizable state as a disulfide bridge [15]. Cys 122 could not be detected because the corresponding peptide was not identified.

4.2. In mitochondria, cysteine over-oxidation is a specific feature of VDACs

The observation that over-oxidation, mainly in VDAC2 and VDAC3, only affects certain cysteines, ensures the absence of artifacts. Oxidation of thiols to sulfonic acid is not attributable to a simple oxidation by air, but, chemically, arises from exposure to strong oxidizing agents such as halogens, hydrogen peroxide, and nitric acid [37]. The presence of oxidative modifications in VDACs could be explained by their localization within the cell, since they are exposed to the intermembrane space (IMS) [15], a cellular compartment where oxidative protein folding occurs [38–40]. Anyhow, despite the existence of a dedicated machinery for the introduction of disulfide bonds, many proteins and protein domains of the IMS contain reduced cysteine residues, probably due to special reductases (i.e. the thioredoxin and the glutaredoxin systems [41–43]). This would primarily explain the carboxyamidomethylated cysteines in VDAC2 and VDAC3 N-terminal regions, likely involved in disulfide bridge formation. What is surprising is the fact that only another mitochondrial protein, found in the HTP eluate, has been identified as sulfonated. It is the mitochondrial matrix protein thiosulfate sulfur-transferase (UniProtKB - P24329) that acts as a mitochondrial import factor for the cytosolic 5S rRNA, involved in the

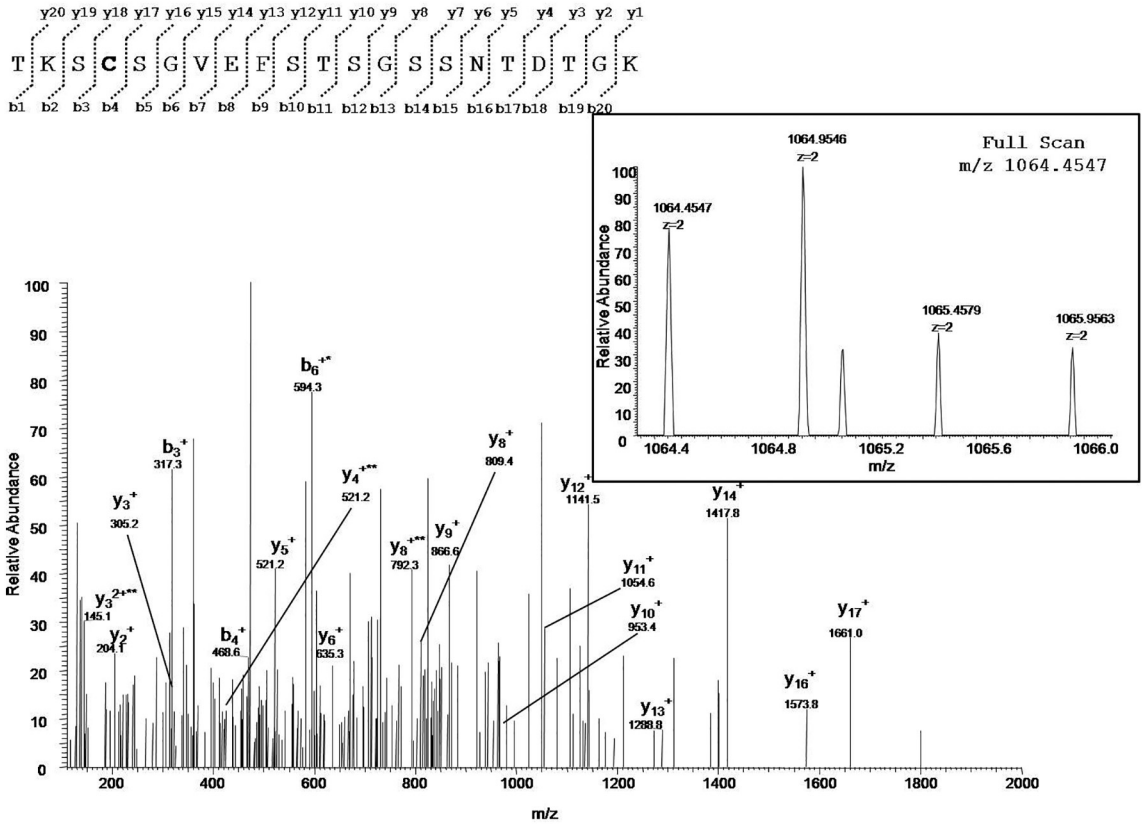

Fig. 4. MS/MS spectrum of the doubly charged molecular ion at *m/z* 1064.4547 (calculated 1064.4530) of the VDAC2 tryptic peptide from *Rattus norvegicus* containing cysteine residue 48 in the form of sulfonic acid. The inset shows the full scan mass spectrum of molecular ion. Fragment ions originated from the neutral loss of H_2O are indicated by an asterisk. Fragment ions originated from the neutral loss of NH_3 are indicated by two asterisks.

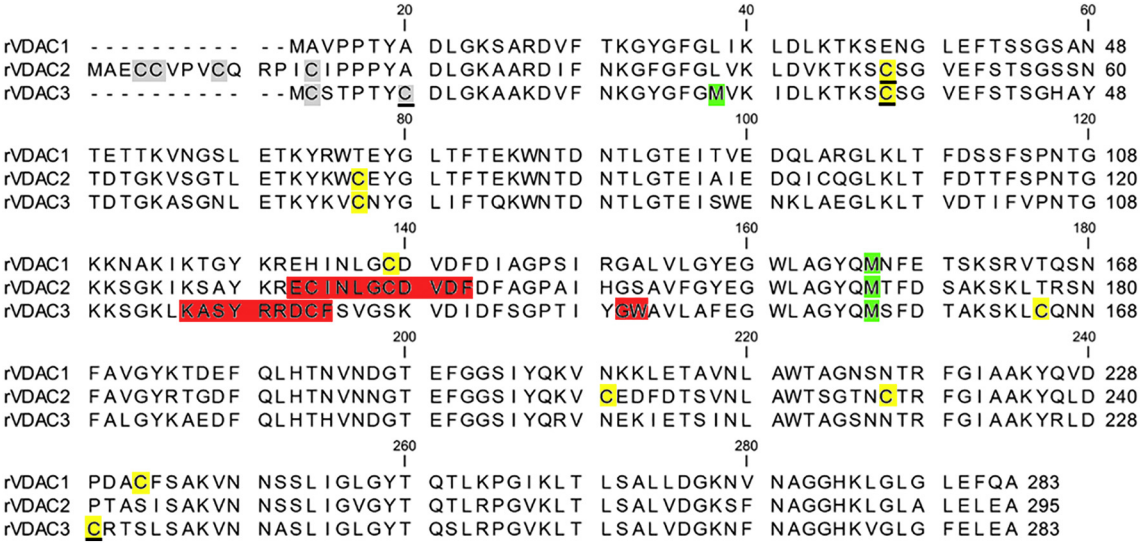

Fig. 5. Multi-alignment of rat VDAC proteins. The cysteine residues identified as carboxamidomethylated are highlighted in gray; the cysteine residues found over-oxidized to sulfonic acid in yellow. In green the methionine residues identified as oxidized; solid lines indicate cysteines identified as succinated. In red the sequences not covered by the mass spectrometric analysis.

Table 3
Comparison of the absolute intensities of molecular ions of a selected sulfur containing chymotryptic peptide found in the analysis of rVDAC2 reduced with DTT, carboxyamidomethylated and digested in-solution.

Peptide	Position in the sequence	Measured monoisotopic *m/z*	Absolute intensity	Ratio Ox/Red
QM**M**TFDSAKSKL	166–176	627.8057 (+2)	$7.91 \cdot 10^4$	3.2
QMTFDSAKSKL		619.8083 (+2)	$2.46 \cdot 10^4$	

M: methionine sulfoxide; **Q**: pyroglutamic acid form.

Table 4
Comparison of the absolute intensities of molecular ions of succinated peptides found in the analysis of rVDAC2 reduced with DTT, carboxyamidomethylated and digested in-solution.

Peptide	Position in the sequence	Measured monoisotopic *m/z*	Absolute intensity	Ratio Succinat/ Norm
TKS**C**SGVEFSTSGSSNTDTGK	45–65	732.6460 (+3)	$2.38 \cdot 10^4$	0.039
TKSCSGVEFSTSGSSNTDTGK		712.9837 (+3)	$6.03 \cdot 10^5$	

C: cysteine succinated.

formation of iron-sulfur complexes, cyanide detoxification or modification of sulfur-containing enzyme and possess a weak mercaptopyruvate sulfurtransferase (MST) activity. This finding defines the sulfonation of cysteine residues as a non-random event that affects specific components and not the entire universe of IMS-exposed mitochondrial proteins. Beside reports that claim the negative effects of such over-oxidations (i.e. the sulfonic acid modification of mammalian Cu, Zn-SOD has been speculated to play an important role in diseases like familial amyotrophic lateral sclerosis [44]), others seem to say otherwise. Lim, J. et al. have indeed shown that sulfonation of a specific residue of Peroxiredoxin activates a "super-chaperone" activity that may be induced during oxidative stress [45].

Moreover, Poderoso and coworkers have demonstrated that the redox state modulates the mitochondrial interaction of MAPKs to MAPKKs by oxidation of conserved cysteine domains of MAPKs to sulfinic and sulfonic acids [46]. Is it therefore possible that the oxidative modification of cysteine residues is the basis of a fine regulation of VDAC pore-forming activity? Considering the different Cys-oxidized-to-sulfonic-acid/Cys-carboxyamidomethylated ratios of the three isoforms, it is tempting to speculate that the redox state "modulates" the specific activity of each isoform according to the cellular needs. In this regard, we have previously demonstrated that the removal of selected cysteine residues in VDAC3 completely overturned channel activity, providing electrophysiological features similar to those of VDAC1 [15]. Likewise, Sodeoka and co-workers have reported that VDAC3 gating is activated by suppression of specific disulfide bonds within the pore [47].

4.3. The number of cysteine residues in VDAC isoforms increases during evolution: a possible explanation

The number of cysteine residues in VDAC raises from the unicellular eukaryotes (*S. cerevisiae* VDAC isoforms 1 and 2 have only two such

Table 5
Comparison of the absolute intensities of molecular ions of succinated peptides found in the analysis of rVDAC3 reduced with DTT, carboxyamidomethylated and digested in-solution.

Peptide	Position in the sequence	Measured monoisotopic *m/z*	Absolute intensity	Ratio succinat/norm
*C*STPTY**C**DLGK	2–12	701.7790 (2+)	$4.76 \cdot 10^5$	0.29
*C*STPTY***C***DLGK		672.2840 (2+)	$1.63 \cdot 10^6$	
TKS**C**SGVEFSTSGHAYTDTGK	33–53	760.3315 (3+)	$8.09 \cdot 10^4$	0.049
TKS***C***SGVEFSTSGHAYTDTGK		740.6678 (3+)	$1.65 \cdot 10^6$	
YRLD**C**R	225–230	417.2109 (2+)	$6.59 \cdot 10^4$	0.049
YRLD***C***R		441.7159 (2+)	$1.34 \cdot 10^6$	

* C: N-terminal acetylated; ***C***: cysteine carboxyamidomethylated; **C**: cysteine succinated.

Table 6
List of the mitochondrial membrane proteins present in the hydroxyapatite (HTP) eluate of Triton X-100 lysate that were identified by UHPLC/ESI-MS/MS. In the table the full name, the percentage of sequence coverage, the number of isoforms identified for each protein, the number of unique peptides, the total number of peptides, the molecular weight in KDa and the calculated isoelectric point are reported. Proteins identified by peptides containing cysteines are reported in bold.

Accession number	Description	Coverage	Proteins	Unique peptides	Peptides	MW [kDa]	Calc. pI
Q9Z2L0	Voltage-dependent anion-selective channel protein 1	95.41	1	32	33	30.7	8.54
P81155	Voltage-dependent anion-selective channel protein 2	64.41	1	14	17	31.7	7.49
P35171	Cytochrome c oxidase subunit 7A2	62.65	1	4	4	9.3	10.27
P62078	**Mitochondrial import inner membrane translocase subunit Tim8 B**	50.60	1	4	4	9.3	5.12
Q9R1Z0	Voltage-dependent anion-selective channel protein 3	45.23	1	8	10	30.8	8.70
Q9JJW3	Up-regulated during skeletal muscle growth protein 5	44.83	1	3	3	6.4	9.83
P26772	10 kDa heat shock protein	43.14	1	4	4	10,9	8,92
P11951	Cytochrome c oxidase subunit 6C-2	36.84	1	3	3	8.4	10.07
P00173	Cytochrome b5	31.34	1	3	3	15.3	4.98
Q9WVJ4	Synaptojanin-2-binding protein	26.90	1	4	4	15.8	6.80
P62898	Cytochrome c	22.86	1	3	3	11.6	9.58
Q9WVA1	**Mitochondrial import inner membrane translocase subunit Tim8 A**	22.68	1	2	2	11.0	5.16
P15999	ATP synthase subunit alpha	22.42	1	9	9	59.7	9.19
P13437	**3-ketoacyl-CoA thiolase**	20.15	1	4	4	41.8	7.94
P08011	**Microsomal glutathione S-transferase 1**	18.71	1	3	3	17.5	9.61
P35434	ATP synthase subunit delta	17.26	1	3	3	17.6	5.24
O88498	Bcl-2-like protein 11	12.76	1	2	2	22.0	6.54
P10719	ATP synthase subunit beta	10.78	1	4	4	56.3	5.34
P63039	60 kDa heat shock protein	8.73	1	4	4	60.9	6.18
Q66H15	Regulator of microtubule dynamics protein 3	7.86	1	3	3	52.3	5.02
P97521	Mitochondrial carnitine/acylcarnitine carrier protein	6.31	1	2	2	33.1	9.48
Q09073	ADP/ATP translocase 2	5.70	1	2	2	32.9	9.73
P22791	Hydroxymethylglutaryl-CoA synthase	5.31	1	3	3	56.9	8.68
Q5BJQ0	Atypical kinase ADCK3	4.31	1	2	2	72.2	6.46
P07756	Carbamoyl-phosphate synthase [ammonia]	3.53	1	4	4	164.5	6.77
Q64428	Trifunctional enzyme subunit alpha	3.28	1	2	2	82.6	9.06

residues) through less evolved animals (zebrafish has only one cysteine in the sequence of VDAC2) to mammalians, where there is the largest number of cysteines.

The functional relevance of cysteine oxidation remains untested in all but a few case: as with other posttranslational modifications, just because a cysteine is oxidized doesn't necessarily mean it plays a functional role. Sulfonic acid (RSO_3H) definitely represents a special issue. Due to resonance in the conjugate base, it can stabilize its negative charge and is comparable in strength to sulfuric acid. There are no known enzymes that can reverse this form back to any of the

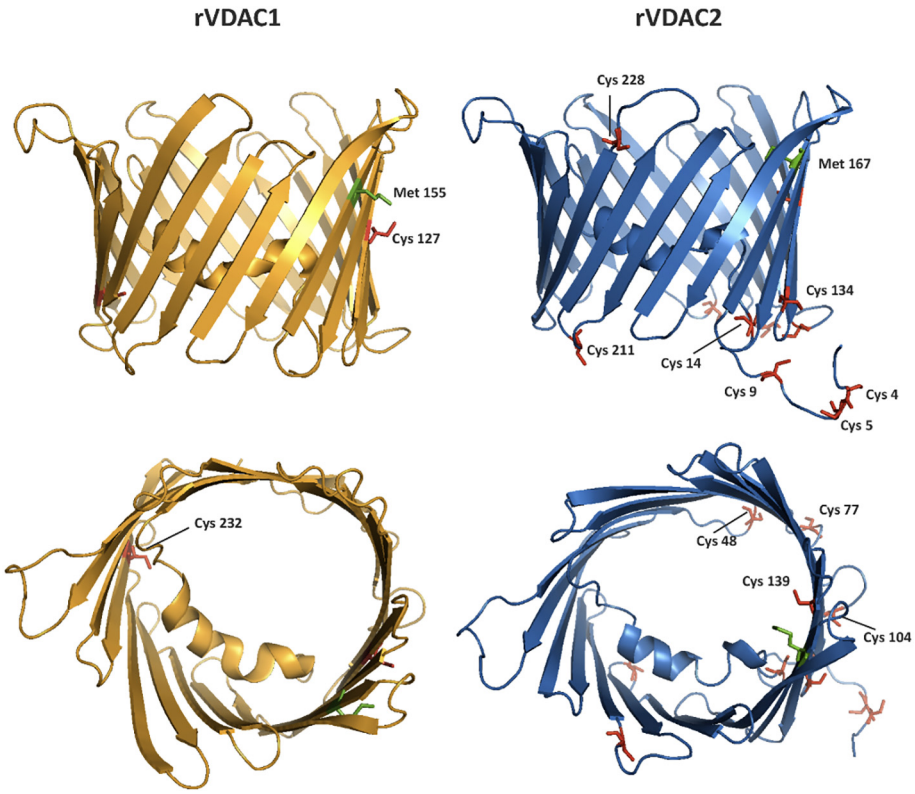

Fig. 6. Side and top views of rat VDAC1 and rat VDAC2 where the cysteine positions have been indicated. The structures are predicted by homology modelling, using mVDAC1 structure (pdb: 3EMN) as a template.

previous sulfur oxidative states (sulfenic and sulfinic forms) and it is suggested to play a role in either inhibiting proteins or targeting them for degradation [48]. In particular, the sulfonic acid group would act as a marker for ubiquitin-dependent protein degradation when formed on an N-terminal cysteine residue, such as in GTPase-activating proteins (the so-called "N-end rule pathway") [49]. In light of this, it is important to point out that in VDAC3, the N-terminal cysteine residue Cys 2 has always been found reduced, together with the nearby Cys 8 [32]. The same with regard to the N-terminal cysteines of the isoform 2 (residues Cys 4, 5, 9 and 14), always identified in the carboxyamidomethylated form. The over-oxidation to sulfonic acid observed, to varying degrees, for all the remaining residues of VDAC2 and VDAC3 and for the Cys 127 and 232 of VDAC1, should therefore assume a totally different meaning and have a presumable regulatory function.

4.4. Cysteine succination in VDAC

In this work it is also reported the identification of succinated cysteines in VDAC2 and VDAC3, but not in VDAC1. Succination is an irreversible post-translational modification that occurs when fumarate reacts with cysteine residues to generate S-(2-succino)-cysteine (2SC). Increased protein succination arises from elevated fumarate concentrations as a result of Krebs cycle inhibition, as observed in some mitochondrial diseases [50], cancer (with fumarate hydratase (FH)-deficiency) [51] and diabetes [52]. Interestingly, in the brainstem of a mouse model of Leigh syndrome, MS/MS analysis identified VDAC1 and VDAC2 as specific targets of succination: in particular, Cys77 and Cys48 were identified as endogenous sites of succination in VDAC2. Authors speculated that cysteine succination of VDAC decreases ATP synthesis in mitochondria, further worsening the already compromised mitochondrial function [50].

5. Conclusions

Our results demonstrate that the mitochondrial rVDAC1 and rVDAC2, in physiological state, contain methionines oxidized to methionine sulfoxide. Furthermore, cysteines 127 and 232 in rVDAC1, and 48, 77, 104, 211, and 228 in rVDAC2, respectively, are oxidized to sulfonic acid in relatively small amount respect to rVDAC3. The peculiar behavior of Met and Cys residues of VDACs may be related with the location of this proteins in a strongly oxidizing environment and may be connected with the regulation of the activity of these trans-membrane pore proteins. The structural features elucidated by the present work may be helpful for a better understanding of the functional role of VDACs 1 and 2.

Authors contributions

RS and MGGP produced the MS analysis; SR, MGGP, AM the biochemical experiments; VC analyzed the selenocysteine occurrence; VDP and SF designed the work and wrote the paper.

Conflict of interest

The authors declare that they have no conflicts of interest with the contents of this article.

Transparency document

The Transparency document associated with this article can be found, in the online version.

Acknowledgements

This work was supported by the Italian Ministero dell'Istruzione, dell'Università e della Ricerca, MIUR, (PRIN project 2015795S5W_005), by the FIR-UNICT 350 CD1 project 2017 to VDP and by a grant from PO FERS 2007/13 4.1.2.A, project "Piattaforma regionale di ricerca traslazionale per la salute". The authors gratefully acknowledge the Bionanotech Research and Innovation Tower (BRIT, PON project financed by the Italian Ministry for Education, University and Research, MIUR) for the availability of the Orbitrap Fusion mass spectrometer. A. Magrì has been recipient of an Umberto Veronesi fellowship. The authors thank dr. Stefano Conti Nibali for his valuable help in the analysis of structural features of VDAC isoforms.

Appendix A. Supplementary data

Supplementary data to this article can be found online at https://doi.org/10.1016/j.bbabio.2018.06.007.

References

[1] R. Benz, Permeation of hydrophilic solutes through mitochondrial outer membranes: review on mitochondrial porins, Biochim. Biophys. Acta 1197 (1994) 167–196.
[2] V. Shoshan-Barmatz, V. De Pinto, M. Zweckstetter, Z. Raviv, N. Keinan, N. Arbel, VDAC, a multi-functional mitochondrial protein regulating cell life and death, Mol. Asp. Med. 31 (2010) 227–285.
[3] V. Shoshan-Barmatz, M. Zakar, K. Rosenthal, S. Abu-Hamad, Key regions of VDAC1 functioning in apoptosis induction and regulation by hexokinase, Biochim. Biophys. Acta 1787 (2009) 421–430.
[4] E.N. Maldonado, K.L. Sheldon, D.N. DeHart, J. Patnaik, Y. Manevich, D.M. Townsend, S.M. Bezrukov, T.K. Rostovtseva, J.J. Lemasters, Voltage-dependent anion channels modulate mitochondrial metabolism in cancer cells: regulation by free tubulin and erastin, J. Biol. Chem. 288 (2013) 11920–11929.
[5] K.L. Sheldon, P.A. Gurnev, S.M. Bezrukov, D.L. Sackett, Tubulin tail sequences and post-translational modifications regulate closure of mitochondrial voltage-dependent anion channel (VDAC), J. Biol. Chem. 290 (2015) 26784–26789.
[6] C. Schwarzer, S. Barnikol-Watanabe, F.P. Thinnes, N. Hilschmann, Voltage-dependent anion-selective channel (VDAC) interacts with the dynein light chain Tctex1 and the heat-shock protein PBP74, Int. J. Biochem. Cell Biol. 34 (2002) 1059–1070.
[7] X. Xu, J.G. Forbes, M. Colombini, Actin modulates the gating of *Neurospora crassa* VDAC, J. Membr. Biol. 180 (2001) 73–81.
[8] T.K. Rostovtseva, P.A. Gurnev, O. Protchenko, D.P. Hoogerheide, T.L. Yap, C.C. Philpott, J.C. Lee, S.M. Bezrukov, α-Synuclein shows high affinity interaction with voltage-dependent anion channel, suggesting mechanisms of mitochondrial regulation and toxicity in Parkinson disease, J. Biol. Chem. 290 (2015) 18467–18477.
[9] A. Magrì, R. Belfiore, S. Reina, M.F. Tomasello, M.C. Di Rosa, F. Guarino, L. Leggio, V. De Pinto, A. Messina, Hexokinase I N-terminal based peptide prevents the VDAC1-SOD1 G93A interaction and re-establishes ALS cell viability, Sci. Rep. 6 (2016 Oct 10) 34802, , http://dx.doi.org/10.1038/srep34802.
[10] S. Shimizu, M. Narita, Y. Tsujimoto, Bcl-2 family proteins regulate the release of apoptogenic cytochrome c by the mitochondrial channel VDAC, Nature 399 (1999) 483–487.
[11] Y. Shi, J. Chen, C. Weng, R. Chen, Y. Zheng, Q. Chen, H. Tang, Identification of the protein-protein contact site and interaction mode of human VDAC1 EITH Bcl2 family proteins, Biochem. Biophys. Res. Commun. 305 (2003) 989–996.
[12] C.H. Wu, Y.W. Lin, T.F. Wu, J.L. Ko, P.H. Wang, Clinical implication of voltage-dependent anion channel 1 in uterine cervical cancer and its action on cervical cancer cells, Oncotarget 7 (2016) 4210–4225.
[13] E.H. Cheng, T.V. Sheiko, J.K. Fisher, W.J. Craigen, S.J. Korsmeyer, VDAC2 inhibits BAK activation and mitochondrial apoptosis, Science 301 (2003) 513–517.
[14] S. Reina, F. Guarino, A. Magrì, V. De Pinto, VDAC3 as a potential marker of mitochondrial status is involved in cancer and pathology, Front. Oncol. 6 (2016) 264.
[15] S. Reina, V. Checchetto, R. Saletti, A. Gupta, D. Chaturvedi, C. Guardiani, F. Guarino, M.A. Scorciapino, A. Magrì, S. Foti, M. Ceccarelli, A.A. Messina, R. Mahalakshmi, I. Szabo, V. De Pinto, VDAC3 as a sensor of oxidative state of the intermembrane space of mitochondria: the putative role of cysteine residue modifications, Oncotarget 7 (2016) 2249–2268.
[16] S. Hiller, R.G. Garces, T.J. Malia, V.Y. Orekhov, M. Colombini, G. Wagner, Solution structure of the integral human membrane protein VDAC-1 in detergent micelles, Science 321 (2008) 1206–1210.
[17] M. Bayrhuber, T. Meins, M. Habeck, S. Becker, K. Giller, S. Villinger, C. Vonrhein, C. Griesinger, M. Zweckstetter, K. Zeth, Structure of the human voltage-dependent anion channel, Proc. Natl. Acad. Sci. U. S. A. 105 (2008) 15370–15375.
[18] R. Ujwal, D. Cascio, J.P. Colletierc, S. Fahama, J. Zhanga, L. Toro, P. Ping, J. Abramson, The crystal structure of mouse VDAC1 at 2.3 A resolution reveals mechanistic insights into metabolite gating, Proc. Natl. Acad. Sci. U. S. A. 105 (2008) 17742–17747.
[19] M.F. Tomasello, F. Guarino, S. Reina, A. Messina, V. De Pinto, The voltage-dependent anion selective channel 1 (VDAC1) topography in the mitochondrial outer membrane as detected in intact cell, PLoS One 8 (2013) e81522.
[20] J. Schredelseker, A. Paz, C.J. López, C. Altenbach, C.S. Leung, M.K. Drexler, J.N. Chen, W.L. Hubbell, J. Abramson, High resolution structure and double

electron-electron resonance of the zebrafish voltage-dependent anion channel 2 reveal an oligomeric population, J. Biol. Chem. 289 (2014) 12566–12577.
[21] C. Martel, Z. Wang, C. Brenner, VDAC phosphorylation, a lipid sensor influencing the cell fate, Mitochondrion 19 (2014) 69–77.
[22] Yu, H., Diao, H., Wang, C., Lin, Y., Yu, F., Lu, H., Xu, W., Li, Z., Shi, H., Zhao, S., Zhou, Y., Zhang, Y. Acetylproteomic analysis reveals functional implications of lysine acetylation in human spermatozoa (sperm). Mol. Cell. Proteomics, 2015, 14, 1009–23. 2015.
[23] M. Yang, A.K. Camara, B.T. Wakim, Y. Zhou, A.K. Gadicherla, W.M. Kwok, D.F. Stowe, Tyrosine nitration of voltage-dependent anion channels in cardiac ischemia-reperfusion: reduction by peroxynitrite scavenging, Biochim Biophys Acta 1817 (2012) 2049–2059.
[24] R. Gupta, Phosphorylation of rat brain purified mitochondrial voltage-dependent anion channel by c-Jun N-terminal kinase-3 modifies open-channel noise, Biochem. Biophys. Res. Commun. 490 (2017) 1221–1225.
[25] Y. Chen, W.J. Craigen, D.J. Riley, Nek1 regulates cell death and mitochondrial membrane permeability through phosphorylation of VDAC1, Cell Cycle 8 (2009) 257–267.
[26] S. Yuan, Y. Fu, X. Wang, H. Shi, Y. Huang, X. Song, L. Li, N. Song, Y. Luo, Voltage-dependent anion channel 1 is involved in endostatin-induced endothelial cell apoptosis, FASEB J. 22 (2008) 2809–2820.
[27] J. Kerner, K. Lee, B. Tandler, C.L. Hoppel, VDAC proteomics: post-translation modifications, Biochim Biophys Acta 1818 (2012) 1520–1525.
[28] C. Martel, M. Allouche, D.D. Esposti, E. Fanelli, C. Boursier, C. Henry, J. Chopineau, G. Calamita, G. Kroemer, A. Lemoine, C. Brenner, Glycogen synthase kinase 3-mediated voltage-dependent anion channel phosphorylation controls outer mitochondrial membrane permeability during lipid accumulation, Hepatology 57 (2013) 93–102.
[29] L. Lefièvre, Y. Chen, S.J. Conner, J.L. Scott, S.J. Publicover, W.C. Ford, C.L. Barratt, Human spermatozoa contain multiple targets for protein S-nitrosylation: an alternative mechanism of the modulation of sperm function by nitric oxide? Proteomics 7 (2007) 3066–3084.
[30] A.H. Chang, H. Sancheti, J. Garcia, N. Kaplowitz, E. Cadenas, D. Han, Respiratory substrates regulate S-nitrosylation of mitochondrial proteins through a thiol-dependent pathway, Chem. Res. Toxicol. 27 (2014) 794–804.
[31] M. Schieber, N.S. Chandel, ROS function in redox signaling and oxidative stress, Curr. Biol. 24 (2014) 453–462.
[32] R. Saletti, S. Reina, M.G. Pittalà, R. Belfiore, V. Cunsolo, A. Messina, V. De Pinto, S. Foti, High resolution mass spectrometry characterization of the oxidation pattern of methionine and cysteine residues in rat liver mitochondria voltage-dependent anion selective channel 3 (VDAC3), Biochim. Biophys. Acta 1859 (2017) 301–311.
[33] V. De Pinto, G. Prezioso, F. Palmieri, A simple and rapid method for the purification of the mitochondrial porin from mammalian tissues, Biochim. Biophys. Acta 905 (1987) 499–502.
[34] D. Ben-Hail, V. Shoshan-Barmatz, Purification of VDAC1 from rat liver mitochondria, Cold Spring Harb Protoc 2014 (2014) 94–99.
[35] A.M. Distler, J. Kerner, S.M. Peterman, C.L. Hoppel, A targeted proteomic approach for the analysis of rat liver mitochondrial outer membrane proteins with extensive sequence coverage, Anal. Biochem. 356 (2006) 18–29.
[36] Z.Q. Guan, N.A. Yates, R. Bakhtiar, Detection and characterization of methionine oxidation in peptides by collision-induced dissociation and electron capture dissociation, J. Am. Soc. Mass Spectrom. 14 (2003) 605–613.
[37] R.J. Cremlyn, An Introduction to Organosulfur Chemistry, John Wiley & Sons, Inc, 1996.
[38] B. Grumbt, V. Stroobant, N. Terziyska, L. Israel, K. Hell, Functional characterization of Mia40p, the central component of the disulfide relay system of the mitochondrial intermembrane space, J. Biol. Chem. 282 (2007) 37461–37470.
[39] L. Banci, I. Bertini, C. Cefaro, S. Ciofi-Baffoni, A. Gallo, M. Martinelli, D.P. Sideris, N. Katrakili, K. Tokatlidis, MIA40 is an oxidoreductase that catalyzes oxidative protein folding in mitochondria, Nat. Struct. Mol. Biol. 16 (2009) 198–206.
[40] A. Chatzi, P. Manganas, K. Tokatlidis, Oxidative folding in the mitochondrial intermembrane space: A regulated process important for cell physiology and disease, Biochim. Biophys. Acta 2016 (1863) 1298–1306.
[41] F.N. Vögtle, J.M. Burkhart, S. Rao, C. Gerbeth, J. Hinrichs, J.C. Martinou, A. Chacinska, A. Sickmann, R.P. Zahedi, C. Meisinger, Intermembrane space proteome of yeast mitochondria, Mol. Cell. Proteomics 11 (2012) 1840–1852.
[42] K. Kojer, V. Peleh, G. Calabrese, J.M. Herrmann, J. Riemer, Kinetic control by limiting glutaredoxin amounts enables thiol oxidation in the reducing mitochondrial intermembrane space, Mol. Biol. Cell 26 (2015) 195–204.
[43] M. Cardenas-Rodriguez, K. Tokatlidis, Cytosolic redox components regulate protein homeostasis via additional localization in the mitochondrial intermembrane space, FEBS Lett. 591 (2017) 2661–2670.
[44] N. Fujiwara, M. Nakano, S. Kato, D. Yoshihara, T. Ookawara, H. Eguchi, N. Taniguchi, K. Suzuki, Oxidative modification to cysteine sulfonic acid of Cys111 in human copper-zinc superoxide dismutase, J. Biol. Chem. 282 (2007) 35933–35944.
[45] J.C. Lim, H.I. Choi, Y.S. Park, H.W. Nam, H.A. Woo, K.S. Kwon, Y.S. Kim, S.G. Rhee, K. Kim, H.Z. Chae, Irreversible oxidation of the active-site cysteine of peroxiredoxin to cysteine sulfonic acid for enhanced molecular chaperone activity, J. Biol. Chem. 283 (2008) 28873–28880.
[46] S. Galli, V.G. Antico Arciuch, C. Poderoso, D.P. Converso, Q. Zhou, E. Bal de Kier Joffé, E. Cadenas, J. Boczkowski, M.C. Carreras, J.J. Poderoso, Tumor cell phenotype is sustained by selective MAPK oxidation in mitochondria, PLoS One 3 (2008) e2379.
[47] M. Okazaki, K. Kurabayashi, M. Asanuma, Y. Saito, K. Dodo, M. Sodeoka, VDAC3 gating is activated by suppression of disulfide-bond formation between the N-terminal region and the bottom of the pore, Biochim. Biophys. Acta 1848 (2015) 3188–3196.
[48] K.G. Reddie, K.S. Carroll, Expanding the functional diversity of proteins through cysteine oxidation, Curr. Opin. Chem. Biol. 12 (2008) 746–754.
[49] T. Tasaki, Y.T. Kwon, The mammalian N-end rule pathway: new insights into its components and physiological roles, Trends Biochem. Sci. 32 (2007) 520–528.
[50] G.G. Piroli, A.M. Manuel, A.C. Clapper, M.D. Walla, J.E. Baatz, R.D. Palmiter, ... N. Frizzell, Succination is increased on select proteins in the brainstem of the NADH dehydrogenase (ubiquinone) Fe-S protein 4 (Ndufs4) knockout mouse, a model of Leigh syndrome, Mol. Cell. Proteomics 15 (2016) 445–461.
[51] P.J. Pollard, J.J. Briere, N.A. Alam, J. Barwell, E. Barclay, N.C. Wortham, T. Hunt, M. Mitchell, S. Olpin, S.J. Moat, I.P. Hargreaves, S.J. Heales, Y.L. Chung, J.R. Griffiths, A. Dalgleish, J.A. Mcgrath, M.J. Gleeson, S.V. Hodgson, R. Poulsom, P. Rustin, I.P.M. Tomlinson, Accumulation of Krebs cycle intermediates and over-expression of HIF1α in tumours which result from germline FH and SDH mutations, Hum. Mol. Genet. 14 (2005) 2231–2239.
[52] J.S. Isaacs, Y.J. Jung, D.R. Mole, S. Lee, C. Torres-Cabala, Y.L. Chung, M. Merino, J. Trepel, B. Zbar, J. Toro, P.J. Ratcliffe, W.M. Linehan, L. Neckers, HIF overexpression correlates with biallelic loss of fumarate hydratase in renal cancer: novel role of fumarate in regulation of HIF stability, Cancer Cell 8 (2005) 143–153.